Application of In-situ Produced Cosmogenic ^{10}Be and ^{26}Al for Estimating Erosion Rate and Exposure Age of Tor and Block Stream Detritus: Case Study from Mt. *Maneo*, South Korea*

Yeong Bae Seong** and Jong Wook Kim***

우주기원 방사성 핵종을 이용한 만어산 암설지형의 침식률 및 노출연대 측정*

성영배** · 김종욱***

Abstract : CRN (Cosmogenic radionuclide) methodology has been a versatile tool applicable to a wide range of geomorphology. This study was undertaken to ascertain the rate of erosion and exposure age of mountain-top detritus (tors and block streams) on Mt. *Maneo* by employing the concentrations of in-situ produced cosmogenic ^{10}Be and ^{26}Al from bedrock surfaces that are exposed to cosmic rays. The results suggest that tors on the summit were positioned here during the glacial period but no later than 65ka and block streams have been stabilized also since the last glacial period but no later than 38ka. The tors on the summit have been eroded at a slower rate (9m/Ma) than blocks on the hillslope (15m/Ma) since the initial abrupt exposure of each landform to cosmic rays, suggesting that there is a slight difference in the rate of erosion between the summit and the hillslope, and that the local relief between the two areas has been increased. When the ^{26}Al/^{10}Be-^{10}Be concentrations from samples are plotted in Lal's steady-state erosion island, one sample (from a tor) has complex exposure histories, which can be explained by the occurrence of multiple chipping events of 5cm to 60cm in length on the surface of the rock.

Key Words : CRN (Cosmogenic radionuclide), Tor, Block stream, Exposure Age, Steady-state erosion, Erosion Rate.

요약 : 우주 기원의 방사성 핵종(核種)은 근래에 지형연구에 널리 활용되고 있다. 본 연구에서는 우주 기원의 방사성 핵종인 ^{10}Be과 ^{26}Al를 이용하여 만어산의 토르와 암괴류를 대상으로 그 구성 암석의 지표 노출 연대와 침식률을 측정하였다. 연구 결과, 토르는 적어도 약 6만 5천년 전, 그리고 암괴류는 적어도 3만 8천년 전에 노출된 것으로 나타났다. 한편, 토르와 암괴류의 구성 암석의 표면 침식률은 각각 9m/Ma, 15m/Ma인 것으로 나타났다. 이러한 침식률의 차이는 풍화 및 침식에 대한 국지적인 조건이 다르기 때문인 것으로 생각된다. 특이한 점은, 산 정부에 위치한 토르의 구성 암석들 중 일부가 ^{26}Al/^{10}Be과 ^{10}Be를 이용하는 Lal (1991)이 밝힌 정상상태 침식구역 (steady-state erosion island)에서 벗어나 있는데 이것은 이 토르의 표면이 비정상적인 침식의 경로를 겪었다는 것을 의미하며 본 연구에서는 5cm-60cm 정도의 표면이 여러 번 떨어져 나갔다는 것으로 판단된다.

주요어 : 우주기원 방사성 핵종, 토르, 암괴류, 노출 연대, 정상상태 침식, 침식률.

1. Introduction

The term mountain-top detritus refers to the regolith cover that mantles summits and ridges of many mid-latitude mountain ranges (Ballantyne, 1998). This regolith has been named as felsenmeer,

blockmeer, boulder fields, or stone fields (Rea. et al., 1996). Several conflicting hypotheses have been suggested regarding the age and significance of mountain-top detritus in mid-latitude areas. Rea, et al. (1996) suggested that on the basis of the fact that plateau block fields contain clay minerals indicative of prolonged chemical weathering and occupy plateau surfaces of inferred Tertiary age, such detritus may essentially be pre-Pleistocene in origin. An alternative opinion was put forward by Ballantyne and Harris (1997) that mountain-top detritus on mid-latitude mountains reflect breakdown of rock by frost weathering under severe periglacial conditions during Pleistocene cold stages. A third possibility is that plateau block fields and other forms of mountain-top regolith have developed since the downwastage of the last ice sheets, particularly under severe periglacial conditions during the Late Weichselian (Late Pleistocene) Late glacial, with continuous development during Holocene (Dahl, 1966). Others have concluded that mountain-top detritus are of complex origin (Kleman and Borgstrom, 1990). They proposed that block fields of rounded boulders reflect pre-Pleistocene deep chemical weathering, whereas regolith covers of angular detritus were formed under periglacial conditions.

Many opinions in Korea have been suggested about mountain-top detritus landforms since Lautensach (1941) who reported the presence of striped terraces (Streifenboden) and turf-banked terraces (Terrasenboden) around the altitude of 2,000m high on the Mt. Baekdoo. Kim (1966) was suggestive of the fossil involution on the slope of Mt. Acha in Seoul. Kim (1970) proposed that the features such as earth hummocks, thufur, turf-banked terraces on Mt. Halla, formed under the present climate. Chang (1983) argued that cryoplanation terraces underlain by solifluction deposits and block fields at the bottom of a cliff at the Chottae-bong of Mt. Jiri were formed under past cold climate whereas earth hummock and turf-banks are active landforms. Kwon (1979) reported that block streams in Geoje island

were produced by mechanical weathering in cold climate and moved on the slope by frost creep. In contrast Kwon (1988) indicated that all features of boulder streams on Mt. Maneo were eroded from the surface and this regolith was produced in the sub-soil region. In addition he suggested that this boulder formation is of composite origin, not being directly associated with cold climate. Jeon (1995) reported that the block streams and block fields in Mt. Maneo have been formed by polygenetic processes. That is, round core stones were produced in warm climate and transportation of boulders occurred in cold-periglacial climate.

In this study, cosmogenic radionuclides are used to infer the exposure ages of tors and blocks on the mountain slope. These rocks are assumed to have been exposed since Last Glacial period. In-situ production and accumulation of Cosmogenic radionuclides commences when a new surface of bedrock is exposed by an abrupt geomorphic event that removes the upper surface (>>2m) over a short period.

2. The Cosmogenic Nuclide Method

The earth is exposed to cosmic rays that originate from our Sun and the Galactic system. The principal nucleons of the cosmic-ray flux are protons, alpha particles, secondary neutrons, and muons. Cosmogenic nuclides are produced by spallation reactions induced by high energy nucleons, secondary thermal neutron capture reactions, and muon-induced reactions. As the cascade of reactions propagated down through the atmosphere and eventually the upper few meters of the Earth' s crust, the composition of the nuclear particle flux tends to become dominated by neutrons (Fig. 1). Considering the reactions mentioned above, cosmogenic nuclides, which can be found in terrestrial environments, are either of extraterrestrial origin, produced in the atmosphere (so called 'Garden Effect), in-situ,
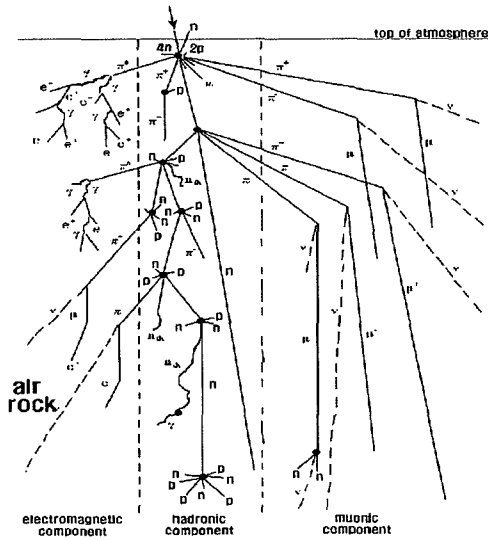
Figure 1. A fate of a primary particle (Tuniz, *et al.*, 1997). The three panels show the different particles generated in the electron, hardron (protons and neutrons), and muon components

of primodial radiogenic, or anthropogenic origin. Over the past decade, the cosmogenic exposure dating method has been undergoing major developments in the wide range of geomorphic areas.

Recent advances in analytical chemistry and unclear physics have provided geomorphologists with the opportunity to constrain rates of landscape

evolution directly. Use of high-sensitivity noble gas and accelerator mass spectrometry (AMS) now allows quantititive abundances measurement of extremely rare isotopes including those produced by the interaction of cosmic rays with rock and soil (Elmore and Phillips, 1987).

The different physical and chemical properties of the six most widely used nuclides (Table 1) make it possible to apply the surface exposure dating methods on rock surfaces of virtually any lithology at any latitude and altitude, for exposures ranging from 10^2 to 10^7 years (Gosse and Phillips, 2001). [10]Be and [26]Al are mostly used because they are produced in quartz, a highly stable and resistant mineral and one of the more common constituents of the lithosphere. The derived nucleons decrease exponentially with depth through the atmosphere, hydrosphere, and lithosphere. A prerequisite for the application of the in-situ produced cosmogenic nuclides for the study of erosional histories of surfaces is knowledge of their production rates under different irradiation conditions: altitude, latitude, irradition geometry and shielding, and erosion rate (Lal, 1991). There have been attempts to refine these production rates (Stone et al., 1998). However, this approach has retained the original estimates for comparative purposes including a 20% error to account for current

Table 1. Principal cosmogenic nuclides and their characteristics in geosciences (modified from Bierman, 1994)

Nuclide	Half-life	Sample Mineral	Characteristics
[3]He	stable	olivine, quartz	- used in extremely long exposure. - diffuse too rapidly.
[10]Be	1.51Ma	quartz, olivine	- chemically prepared with [26]Al, [21]Ne, and ^{14}C in quartz and olivine almost ubiquitous. - [10]B is a significant isobar.
[14]C	5730a	quartz	- excellent for short exposure history. - difficult for chemical pretreatment.
[21]Ne	stable	olivine, quartz	- used in extremely long exposure. - diffuse too rapidly.
[26]Al	0.72Ma	quartz, olivine	- production rate is higher than [10]Be. - difficult to measure quartz with low [26]Al/[27]Al contents
[36]Cl	0.31Ma	whole rock	- useful for erosion and burial investigation due to multiple production pathways. - difficult to decipher individual pathways.

levels of variation.

In common rock (=2.7g cm^{-3}), roughly half the fast cosmic-ray neutrons are absorbed above a depth of 60cm (attenuation length = 150-170g cm^{-2}). The number of atoms of the in-situ produced cosmogenic nuclides (N(x,t)) within the rock at any depth, x, after an irradiation period t (years), is given by the following equation,

$$N(x,t) \equiv N(x,0)e^{-\lambda t} + \frac{p(0)}{\lambda + \rho \varepsilon / \Lambda} e^{-\rho x / \Lambda}(1 - e^{-(\lambda + \rho \varepsilon / \Lambda)t})$$

(Equation 1)

where N(x,0) is the initial number of atoms/g in the rock surface at depth, x, after an irradiation for a time period, t (year). is the attenuation length (g cm^{-2}) for spallogenic production, ρ is the density of target material in g cm^{-3}, ε is the erosion rate in cm y^{-1}, and λ is the disintegration constant in y^{-1}. P(0) is the production rate that depends on altitude and geomagnetic latitude.

Figure 2 shows the concentrations of in-situ produced cosmogenic nuclides for the case where there is no erosion. Radioactive isotopes approach a steady-state concentration after 4 to 5 half-lives, which limits the application of those isotopes to cases where the exposure age is within 3 to 4 half-
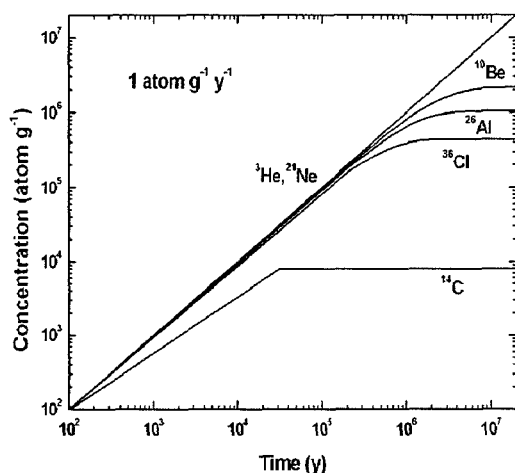

Figure 2. Concentration of in-situ cosmogenic nuclides for the case with no erosion.

lives. For cases where there is significant erosion, steady-state values are reached earlier.

Under favorable circumstances (simple exposure and negligible erosion), a single nuclide may suffice to define the exposure age or erosion rate of a surface (Gillespie and Bierman, 1995). However, in the general case, the measured cosmogenic radionuclide concentration in a sample will be a function of at least two independent variables (exposure age and erosion rate) and in order to determine both of them, therefore, the concentrations of at least two isotopes must be measured. The two-nuclide approach was embodied by Lal (1991). He proposed application of the ^{26}Al/^{10}Be pair, since both can be readily measured in a single mineral separate (quartz), both have similar geochemical behavior, and they have half-lives that differ by a factor of two (T$_{1/2}$ of ^{26}Al is 0.72Ma and T$_{1/2}$ of ^{10}Be is 1.52Ma). The ratio of concentrations of two radionuclides in an eroding surface changes sensitively with the rate of erosion. At steady-state, the ratio of concentrations of two radionuclides at the rock surface is given by the equation:

$$R(^{26}Al/^{10}Be) = N(^{26}Al)/(^{10}Be) = \frac{P(^{26}Al)\lambda_{26Al} + \rho \varepsilon / \Lambda}{P(^{10}Be)\lambda_{10Be} + \rho \varepsilon / \Lambda}$$

$$= \frac{P(^{26}Al)}{P(^{10}Be)} \cdot \frac{1}{(P_{10Be}/N_{10Be}) + \lambda_{26Al} - \lambda_{10Be}}$$

(Equation 2)

Since the ratio of a shorter half-life nuclide to a longer half-life nuclide is considered, the ratio steadily decreases as exposure time increases. The ratio after t years of exposure is then given by:

$$R(t) = \frac{1}{N_{10Be}} \frac{P_{26Al}}{\lambda_{26Al}} \left[1 - \left(1 - N_{10Be} \frac{\lambda_{10Be}}{P_{10Be}}\right)^{\lambda_{26Al}/\lambda_{10Be}} \right]$$

(Equation 3)

3. Study Area and Sample Preparation

The research area is located on Mt. Maneo, southeast Korea that has an elevation of 670.4m. The
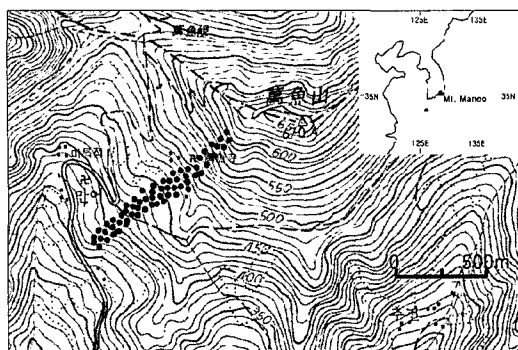
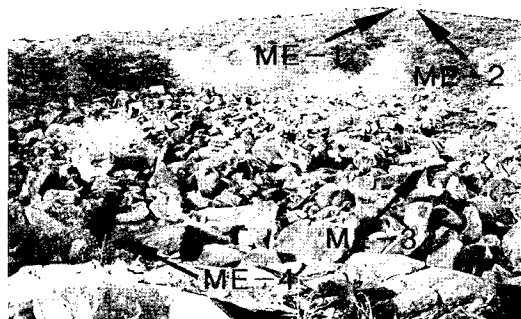Figure 3. Topographical map of study area. Dots represent blockstreams.

Figure 4. Sampling sites

regional slope ranges from less than 5° at the base to over 25° at the summit (Fig. 1). Between the summit and the elevation of 500m, the slope angle exceeds 25°. The slope declines gradually until it makes less than 5° at the altitude of 300m. The significant relief-forming features are mountain-top detritus (tors and block streams) whose origin cannot be explained under the present climate. There are no permanent streams and the landscape is dominated only by bedrock weathering and slope processes. In the study area (Fig. 3), the tors on the summit and the blockstreams (dots) are formed largely of Cretaceous fine-grained granodiorite.

It is known that the neutron-induced production rate of [10]Be or [26]Al is constant within the top 5cm of an exposed surface but then decreases exponentially below this depth (Masarik and Reedy, 1995). It is thus reasonable to only use the top 5cm of rock surface for surface exposure dating. In this study, two categories of materials are sampled and the top 1.5cm of each rock is only used (Fig. 4). Two samples (ME-1, ME-2) are collected from the surface of tors on the summit and the other one is obtained from blocks on the slope. The elevation, latitude, and longitude of sample sites were determined from 1:5,000 topographic maps and Garmin GPS.

The samples were crushed and sieved to a uniform size of 125-250μm. Clean quartz was separated from the rocks by a chemical isolation method (Kohl and Nishiizumi, 1992) using HCl and HF-HNO[3]

baths. An aliquot of the dissolved sample was used to determine the Al content using ICP-MS. A Beryllium carrier and, or stable aluminium carrier when appropriate, was added to the clean quartz separates and the sample was then dissolved in an HF-HNO[3] mixture. The purification of quartz was undertaken at the SNU-AMS laboratory, chemical dissolution and separation and Beryllium-10 AMS measurement were carried out at the Institute of Gelogical and Nuclear Science (IGNS) of New Zealand and aluminium-26 was measured at Lawrence Livermore National Laboratory (LLNL) of USA.

4. Analytical Result and Interpretation

1) Analytical Results and Errors

The analytical results are presented in Table 2. The calculated errors in the concentration of CRN include propagation of uncertainties in the AMS analyses ($\sim \pm 5\%$). stable isotope carrier concentration ($\sim \pm 2\%$), and ICP-MS analyses ($\sim \pm 2\%$). Age errors include uncertainties in sea level, high latitude rate of production ($\pm 10\%$); rock density ($\sim \pm 5\%$); latitude altitude corrections ($\pm 10\%$); and absorption mean free path ($\sim \pm 5\%$). We neglect errors in the rate of production introduced by changes in the intensity of the magnetic field because of current
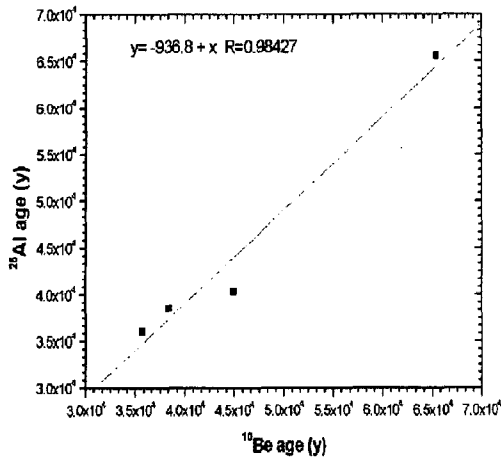
Figure 5. Comparison of ^{10}Be and ^{26}Al effective ages obtained from this study.

uncertainty in the calibrations of the rate of production. The ages presented in Table 2 are derived from equation 1. Figure 5 shows the comparison of ^{10}Be and ^{26}Al ages from 4 samples.

The agreement in exposure ages between ^{10}Be and ^{26}Al samples collected on individual surfaces is favorable (Fig. 5), which indicates that there is good consistency of experimental procedure and data analysis used, and that inheritance of cosmogenic radionuclides is negligible.

2) Maximum Erosion Rate

The measurement of erosion rates, in different geomorphic settings and across various temporal and spatial scales, is essential to the quantification of rates and styles of landscape evolution, the understanding of the controls and efficiencies of different geomorphic processes, and the establishment of connections between climate change and landscape response (Owen, et al., 2001). At present, the analysis of in situ produced cosmogenic radionuclides (CRNs) is the only reliable way to directly quantify the long-term average (> 10^3-10^4yrs) erosion rates of bedrock surfaces. Concentration of cosmogenic nuclide becomes saturated (secular equilibrium) after prolonged steady-state erosion when t >> $1/[\lambda +(\rho\varepsilon/\Lambda)]$. That is, steady-state erosion must have removed a layer of rock equivalent to two or more erosion cosmic-ray attenuation lengths (Λ/ρ). Erosion is in steady state if constant on the time scale of cosmogenic nuclide accumulation (10^4~10^5yrs). Under these circumstances, a measured concentration can be interpreted in terms of a maximum, steady-state erosion rate (Lal, 1991).

$$\varepsilon = \frac{\Lambda}{\rho}\left[\frac{P}{N} - \lambda\right]$$ (Equation 4)

Table 2. ^{10}Be and ^{26}Al data on study samples

Sample	Latitude (°N)	Longitude (°E)	Altitude (km)	Mass of quartz (g)	Al in quartz(ppm)	prodution rate (atoms g⁻¹y⁻¹)	
						^{10}Be	^{26}Al
ME-1	35°27'20'	128°57'20'	0.6704	21.225	166.7	9.002	54.827
ME-2	35°27'20'	128°57'23'	0.6704	27.749	149.8	9.002	54.827
ME-3	35°27'12'	128°57'10'	0.431	21.456	193.5	7.523	45.9
ME-4	35°27'10'	128°57'8'	0.429	22.896	170.3	7.503	45.75

	Concentration (10 atoms g⁻¹ quartz)		Ratio (^{26}Al/^{10}Be)	Erosion rate (mMa⁻¹)		Exposure age (ka)	
	^{10}Be	^{26}Al		^{10}Be	^{26}Al	^{10}Be	^{26}Al
ME-1	4 0.27	21.69±0.73	5.41±0.59	13.61±2.72	15.02±3	44.93±8.9	40.3±8.1
ME-2	5.79±0.22	34.86±1.25	6.01±0.66	9.31±1.86	9.12±1.82	65.37±1.3	65.6±13.1
ME-3	2.86±0.2	17.38±0.67	6.07±0.66	15.95±3.19	15.69±3.13	38.3±7.6	38.5±7.7
ME-4	2.65±0.16	16.2 ±0.64	6.1 ±0.6	17.21±3.44	16.87±3.37	35.6±7.1	36.1±7.2

* Assumes scaling function of Lal(1991), with 3% sea-level ^{10}Be production by muons.

All errors are 1 standard deviation.

Table 3. Erosion rates determined from cosmogenic and Fission Track analysis (modified from Small et al., 1997).

Location	Rock type	Erosion rate	Climate(m Ma¹)	Method	Authors
Mt. Evans(USA)	granite	8	alpine	CRNª	Nishizumi et al., 1993
Himalayas	granodiorite	14	alpine	CRN	Bierman, 1994
Georgia Piedmont	granite	8	temperate	CRN	Bierman, 1993
Alabama Hills	granite	7	semi-arid	CRN	Kurz, 1986
Eyre(Australia)	granite	0.5-1.0	semi-arid	CRN	Bierman and Turner, 1995
Antarctica	sandstone	0.1-1.0	hyper-arid	CRN	Nishizumi et al., 1991
New England Pluton	granite	25-35	temperate	FTᵇ	Bierman, 1994
SE Australia Pluton	granite	30-40	semi-arid	FT	Bishop, 1985
Western USA	Granit, Gneiss	50	temperate	SBᶜ	Small et al., 1997
Mt. Maneo	granodiorite	10-15	temperate	CRN	This study

a: Cosmogenic radionuclides.

b: Fission-Track analysis.

c: Sediment budget analysis.

where ε is the erosion rate in cm y⁻¹, is the macroscopic attenuation length (150-170g cm⁻²) for spallogenic production, ρ is the density in g cm⁻³, P is the production rate in atom g⁻¹y⁻¹, N is the concentration in atom g⁻¹, and λ is decay constant in y⁻¹. Table 3 compares previously reported erosion rates measured from bare bedrock surfaces from different climatic zones with the results of this study. As seen in Table 3, erosion rates span a wide range (0.1-50m/Ma). This variability is not surprising since measurements have been made from various lithologies and in different environments. However, erosion rates determined using CRN method are lower than those of the sediment budget (Small et al., 1997) and fission track methods (Bishop, 1985; Bierman, 1994). In this study, the maximum erosion rate from a tor on the summit (ME-2) is 9.31±.1.86m/Ma and that from blocks in the slope is 17.21±3.44m/Ma (Table 2). Though coming from a limited number of samples, these results suggest that there is a difference in the rate of erosion (or denudation rate) between the summit and the slope, which increases the local relief between two regions.

3) Effective Minimum Exposure Age

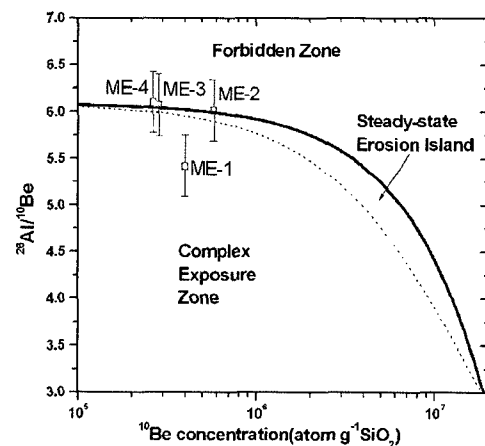The exposure and erosion history of a given sample can be inferred from the position relative to the

Figure 6. "Steady-state Erosion Island" plot of ²⁶Al/¹⁰Be against ¹⁰Be concentration (Lal, 1991). The upper bound of the (solid line is traced by irradiating a rock of zero erosion and the under bound of the curve (dotted line) is drawn by assuming steady-state erosion of a rock.

"Steady-state Erosion Island" (Fig. 6). In this diagram, a sample can be plotted in four fields which provide different information about the age, erosion style and rate, and history of surface burial (Gosse and Phillips, 2001).

(i) Samples with ²⁶Al/¹⁰Be greater than the initial production ratio (plot above the steady-state erosion island) cannot be explained by any combination of

erosion, burial, exposure, or inheritance. The only possible explanations can be issued by radiogenic production of both isotopes and sample preparation or measurement problem.

(ii) Samples which plot on the production ratio curve probably have never been buried or eroded during current exposure duration, and inheritance from an earlier exposure is unlikely. The distance along the production ratio curve corresponds to the exposure age of the sample. The ^{10}Be or ^{26}Al concentration can be interpreted directly as an exposure age. Both isotopes will yield the same exposure age.

(iii) Samples plotting within the steady-state erosion island have traditionally been interpreted to represent some combination of erosion and exposure. A unique production ratio curve for a constant, gradual, and continuous erosion rate can be fit through the sample, so the sample's erosion rate and age (distance along that erosion curve) can be calculated simultaneously. If the two nuclides were interpreted as ages separately, the shorter half-lived isotope will yield a younger age, and the disparity increases with exposure duration.

(iv) Samples plotting below the steady-state erosion island (under the curve that connects all of the end points of the erosion production curves) have traditionally been interpreted as indicating that the exposure of the surface was interrupted by a shielding event (Bierman et al., 1999). When a surface is completely or partially buried (e.g. by snow, sediment, glaciers, or water), the ratio will change due to the differences in the radioactive decay rates of the two isotopes. If the longer-lived isotope is the denominator, the ratio will decrease during burial. Graphically, therefore, the pathway of the buried sample is slightly toward the origin. The length of the path (or distance below the steady-state erosion island) is proportional to the burial duration. Once the burial period is over and the surface becomes exposed again, the ratio will increase (on an exponential pathway toward the production ratio curve). Therefore, ratios plotting below the island have been

interpreted to have undergone complicated exposure histories, where the surface was shielded from cosmic rays at least once.

Three of the samples (ME-2, ME-3, ME-4) show a very close agreement between erosion rates based on ^{10}Be and ^{26}Al and plot, within error limits, inside the "Erosion Island" area. This is consistent with a simple exposure history (Case-iii). However, a complex exposure history cannot be ruled out completely because of large uncertainties. Sample ME-1 displays a more complex exposure history (Case-iv), possibly involving periods of burial or non-steady-state erosion. In the case of the three samples that are viewed as having experienced steady-state erosion (ME-2, ME-3, ME-4), the effective exposure ages obtained from nuclide concentration indicate a minimum exposure age.

On the other hand the effective exposure age of sample ME-1 that has experienced non-steady state erosion implies a minimum age for the subsequent event that occurred after the prior exposure. As mentioned above, from the buried sample alone, there is no way to determine how many episodes of burial or the total duration of burial that a surface may have experienced, and without independent information there is no way to determine how long a surface was exposed since burial (Bierman et al., 1999).

However, there may be two possible geomorphic explanations for the complex exposure history in this case: (i) burial by allochthonous sediments, or (ii) non-steady-state erosion related to local process of mass-wasting. As for burial by sediments transported from another area, the close proximity of buried (ME-1) and continuously exposed sample (ME-2) makes this possibility untenable as an explanation for the complex exposure history of ME-1.

Field observations of our sampled tors and blocks reveal two scales of weathering processes. At the small scale, there is granular disintegration and displacement of thin (<<50mm thick) laminar sheets. At the larger scale, more than 60cm-thick sheets or

blocks, apparently related to subaerial weathering chip off. The coarse fragments are then removed either by rock fall on steep slopes or by gradual creep at lower gradients whereas the fines are ultimately removed by surface wash. Lal (1991) modeled a particular case of non-steady erosion, in which the outcrop erodes at a constant rate before and after a single chip is removed. Directly following the chipping event, the CRN concentration at the surface of the outcrop drops to the steady-state erosion concentration found at the chip depth. The surface CRN concentration subsequently increases until the original steady-state surface concentration is attained.

However, under periglacial or alpine environment where this landform is assumed to be formed, the erosion behavior is more complex than Lal's model (1991). Our field observations indicate that tors and blocks in the study area have been eroded by the episodic removal of finite blocks. Episodic erosion has also been observed in other alpine and periglacial environments. Non-steady-state erosion resulting from the episodic removal of spalling sheets ~60cm thick could also have caused the apparent complexity in erosion history of the ME-2 (Small et al., 1997). A ratio will also plot below the steady-state erosion island if the surface has experienced episodic erosion in which thick layers of material are removed rapidly, such as during subglacial plucking or block erosion of a retreating vertical cliff face (Gosse et al., 1995). On field evidence, it seems likely that complexity in the sample (ME-2) comes from an episodic chipping event. The distance by which the zero-erosion production curve is displaced to the left is proportional to the thickness of the block removed.

5. Conclusion

Our strategically selected samples from measurement on Mt. Maneo yield concentrations of cosmo-

genic ^{10}Be and ^{26}Al that indicate lower erosion rates (~15m/Ma) than other conventional methods and exposure ages (38ka ~ 65ka) compatible with relative datings from other studies (Kwon, 1988; Jeon, 1995). The maximum bedrock erosion rate measured from tors and blockstreams on Mt. Maneo is 10-15m per Ma. These erosion rates are very similar to CRNs erosion rates measured in other environments and the difference between erosion rates at the summit and slope indicates that local relief has been increasing since the last exposure event. The ^{26}Al/^{10}Be ratios suggest that most of the samples studied except ME-1 were exposed in a steady-state environment. The cosmogenic radionuclide data indicate that tors on the summit (ME-1, ME-2) were rapidly exposed no later than 65ka by an abrupt geomorphic event and the blocks (ME-3, ME-4) on the slope were transported from the bedrocks on the summit and stabilized no later than 38ka.

References

Ballantyne, C. K., 1998, Age and significance of mountain-top detritus, *Permafrost and Periglacial Processes*, 9, 327-345.

Bierman, P. R., Marsella, K. A., Patterson, C., Davis, P. T. and Caffe, M., 1999, Mid-southwestern Minnesota and southern Baffin Island: a multiple approach, *Geomorphology*, 27, 25-39.

Bierman, P.R., 1994, Using in situ produced cosmogenic isotopes to estimate rates of landscape evolution: a review from the geomorphic perspective, *Journal of Geophysical Research*, 99(B7), 13885-13896.

Bierman, P.R., 1993, *Cosmogenic Isotopes and the Evolution of Granitic Landforms*, Ph. D. Thesis, University of Washington.

Bishop, P., 1985, Southeast Australian late Mesozoic and Cenozoic denudation rates: a test for late Tertiary increases in continental denudation, *Geology*, 13, 479-482.

Chang, H., 1983, Periglacial landforms in the eastern part of the main ridge of Mt. *Jiri*, South Korea, *Geography*, 27, 31-50. (In Korean)

Clark, M.J., 1988, *Advances in Periglacial Geomorphology*, John Wiley & Sons.

Dixon, J.C. and Abrahams, A.D., 1992, *Periglacial Geomorphology*, John Wiley & Sons.

French, H., 1996, *The Periglacial Environment*, Longman.

Gillespie, A.R., and Bierman, P.R., 1995, Precision of terrestrial exposure ages and erosion rates estimated from analysis of cosmogenic isotopes produced in situ, *Journal of Geophysical Research*, 24, 637-649.

Gosse, C.J. and Phillips, F.M., 2001, Terrestrial in situ cosmogenic nuclides: theory and application, *Quaternary Science Reviews*, 20, 1475-1560.

Granger, D.E., Kirchner, J.W. and Finkel, R., 1996. Spatially averaged long-term erosion rates measured from in situ-produced cosmogenic nuclides in alluvial sediment, *Journal of Geology*, 104, 249-257.

Jeon, Y. K., 1995, A study on the block streams in Mt. *Maneo*, *Journal of Korean Geomorphological Association*, 2(1), 43-56. (In Korean)

Kim, D. J., 1970, Patterned ground of Mt. *Halla*, *Naksan Geography*, 1, 3-10. (In Korean)

Kim, K., 2001, *Understanding Cosmogenic Nuclide Production Underground*, Ph. D. Thesis, University of Victoria, New Zealand.

Kleman, J. and Borgstrom, I., 1994, Preservation of landforms under ice sheets and ice caps, *Geomorphology*, 9, 19-32.

Kohl, C. P. and Nishiizumi, K., 1992, Chemical isolation of quartz for measurement of in-situ produced cosmogenic nuclides, *Geochimica et Cosmochimica Acta*, 56, 3583-3587.

Kwon, S. S., 1979, Fossil periglacial phenomena on the southern parts of *Geoje* island, Korea, *Journal of Geography*, 6, 151-153. (In Korean)

Kwon, S. S., 1988, On the accumulated granite boulders of the Mt. *Maneo*, Korea, *Journal of*

Geography, 15, 29-44. (In Korean)

Lal, D., 1991, Cosmic ray labeling of erosion surfaces: in-situ nuclide production rates and erosion models, *Earth and Planetary Science Letters*, 104, 424-439.

Lautensach, 1941, *Korea*, Springer-Verlag.

Masarik and Reedy, 1995, Terrestrial cosmogenic-nuclide production systematics calculated from numerical simulations, *Earth and Planetary Sciences Letters*, 136, 381-395.

Nishiizumi, K., Klein, J., Middleton, R., and Craig, H., 1990, Cosmogenic [10]Be and [26]Al and [3]He in olivine from Maui lavas, *Earth and Planetary Science Letters*, 98, 263-266.

Nishiizumi, K., Kohl, C.P., Shoemaker, E.M., Arnold, J.R., Klein, J., *et al.*, 1991, In situ [10]Be and [26]Al exposure ages at Meteor Crater, Arizona, *Geochimica et. Cosmochimica Acta*, 55, 2699-2703.

Nishiizumi, K., Lal, D., Klein, J., Middleton, R., and Arnold, J. R., 1989, Cosmic ray production rates of [10]Be and [26]Al in quartz from glacially polished rocks, *Journal of Geophysical Research*, 94(17), 17907-17915.

Oguchi, T. and Tanaka, Y., 1998, Occurrence of extrazonal periglacial landforms in the lowlands of western Japan and Korea, *Permafrost and Perigalcial Processes*, 9, 285-294.

Owen, L.A., Gualtieri, Finkel, R.C., Caffee, M., Benn, D.I., and Sharma, M., 2001, Cosmogenic radionuclide dating of glacial landforms in the Lahul Himalaya, northern India: defining the timing of Late Quaternary glaciation, *Journal of Quaternary Science*, 16(6), 555-563.

Rea, B. R., Whalley, W. B., Rainey, M. M., and Gordon, J. E., 1996, Blockfields, old or new? Evidence and implications from some plateaus in northern Norway, *Geomorphology*, 15, 109-121.

Repka, J.L., Anderson, R.S. and Finkel, R.C., 1997, Cosmogenic dating of fluvial terraces, Fremont River, Utah, *Earth and Planetary*

Science Letters, 152, 59-73.

Small, E.E., Anderson, R.S., Repka, J.L. and Finkel, R., 1997. Erosion rates of alpine bedrock summit surfaces deduced from in situ ¹⁰Be and ²⁶Al, *Earth and Planetary Science Letters,* 150(3-4), 413-425.

Stone, J. O., Ballantyne, C. K., and Fifield, L. K., 1998, Exposure dating and validation of periglacial weathering limits, Northwest Scotland, *Geology,* 26(7), 587-590.

Summerfield, M. A., Stuart, F. M., Cockburn, H. A. P., Sudgen, D. E., Denton, G. H., Dunai, T., and Marchant, D. R., 1999, Long-term rates of denudation in the dry valleys, transantarctic mountains, southern Victoria Land, Antarctica based on in-situ-produced cosmogenic ²¹Ne, *Geomorphology,* 27, 113-129.

Tuniz, C., Bird, J., Fink, D. and Herzog, G., 1998, *Accelerator Mass Spectrometry,* CRC.